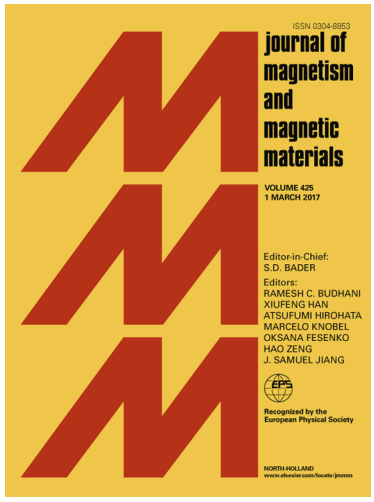

Towards magnetic monopole interaction measurement in artificial spin ice systems

J.H. Rodrigues, L.A.S. Mól

PII: S0304-8853(17)32948-7
DOI: https://doi.org/10.1016/j.jmmm.2018.03.032
Reference: MAGMA 63803

To appear in: *Journal of Magnetism and Magnetic Materials*

Received Date: 15 September 2017
Revised Date: 21 February 2018
Accepted Date: 15 March 2018

Please cite this article as: J.H. Rodrigues, L.A.S. Mól, Towards magnetic monopole interaction measurement in artificial spin ice systems, *Journal of Magnetism and Magnetic Materials* (2018), doi: https://doi.org/10.1016/j.jmmm.2018.03.032

Towards magnetic monopole interaction measurement in artificial spin ice systems

J. H. Rodrigues[a,b], L. A. S. Mól [a,*]

[a]*Laboratório de Simulação, Departamento de Física, ICEx*
Universidade Federal de Minas Gerais, 31720-901 Belo Horizonte, Minas Gerais, Brazil
[b]*Núcleo de Física, Instituto Federal de Minas Gerais - Campus Bambuí, 38900-000, Bambuí, Minas Gerais, Brazil*

Abstract

In this paper we seek for detectable modifications in system properties induced by the Coulombian interactions between magnetic monopoles in an artificial spin ice system as an attempt to provide theoretical support to experiments devoted to measure the magnetic charge of monopole excitations. To this end an emergent vertex model was developed, validated and afterwards used to explore Coulombian interaction modifications on the distribution of monopole-like excitations in a magnetization reversal process. Our results show that the analysis of the skewness and kurtosis of the distribution of monopoles can be used to identify the presence of Coulombian interactions. These results are shown to be robust against the presence of disorder and temperature fluctuations.

Keywords:
Magnetic monopoles; Artificial Spin ice; Dumbbell model; Vertex model
PACS: 05.10.Ln, 75.10.Hk, 75.78.-n

1. Introduction

Spin ice [1, 2] is a class of frustrated magnetic materials which exhibit disorder in the configuration of magnetic moments similar to that found in the water ice. Its crystalline structure is such that magnetic moments are placed at the corners of a lattice of corner sharing tetrahedra, the pyrochlore lattice, being dysprosium titanate ($Dy_2Ti_2O_7$) and holmium titanate ($Ho_2Ti_2O_7$) its main examples. In these compounds, a strong single ion anisotropy enforce magnetic moments to point along the direction that connects the center of adjacent tetrahedra, in such a way that due to the frustrated magnetic and exchange couplings configurations where two spins point inward and two outward at each vertex are favored. Then, the system's ground state is degenerated and follows the "two-in", "two-out" ice rule in each vertex. In 2008, Castelnovo et al [3] realized that excitations above the degenerated ground state, generated by the ice rule violation, could be interpreted as emergent quasiparticles that behave like magnetic monopoles, being the first example of fractionalization in a three dimensional system. However, proper sampling of individual magnetic moments in a spin ice crystal is not possible with current experimental techniques. As a way to circumvent this difficulty, allowing more detailed analysis of frustration effects, Wang et al [4, 5] proposed that a lattice of elongated magnetic nanoislands that mimics some of the basic ingredients of spin ice compounds, the artificial spin ice (ASI), could be used to study frustration effects in magnetic systems.

Besides the possibility of sampling individual magnetic moments in a lattice of interacting magnets by techniques such as Magnetic Force Microscopy (MFM) and X-Ray Magnetic Circular Dichroism (XMCD), the kind of system proposed in Wang's seminal work also allow the study of any kind of arrangement of magnetic dipoles in two dimensions [5]. Indeed, their proposal is based on a lattice of lithographically built elongated nanoislands, each one approximately described as an Ising-like dipole, in such a way that any two dimensional arrangement of these building blocks can be built. Because of that, each geometry of artificial spin ice is unique and each of them have different physical properties. For example, among many different realizations to date, the square lattice [4] is the one that most resembles the crystalline spin ice since each vertex has four dipoles that may point inward or outward and ice rule satisfying configurations are favored; the honeycomb (kagome) lattice [6, 7] is related to a planar mapping of the pyrochlore lattice and have only three spins at each vertex; the triangular lattice is the one that has a simple way to achieve the ground state through a uni-directional magnetic field [8, 9]; just to name a few. In addition, most of these systems also have as low energy excitations quasi-particles that behave as magnetic monopoles [8, 10, 11, 12, 13].

Concerning monopole-like excitations in these systems, some aspects should be remarked. In the crystalline spin ice (CSI) Castelnovo et al [3] showed that magnetic monopoles emerge as elementary excitations by using a dumbbell model, where each dipole (spin) is replaced by a dumbbell of magnetic charges separated by the diamond lattice spacing. Then, configurations violating the ice-rule generate vertices with a net magnetic charge that interacts via Coulombian interactions. Since the dumbbell model reproduces system's energy up to terms

*Corresponding author
Email addresses: joao.henrique@ifmg.edu.br (J. H. Rodrigues), lucasmol@fisica.ufmg.br (L. A. S. Mól)

proportional to $1/r^5$ proper description of system's properties is obtained by this simplified model. However, the same is not so simple for the ASI systems [14]. Indeed, a simple resummed dumbbell model is not capable of reproduce the system's energy, in such a way that the monopoles concept cannot be readily translated to this system. The main difference is that while in the pyrochlore lattice all vertices satisfying the ice rule have the same intrinsic dipole moment, in the artificial spin ice in a square lattice, vertices on topology T_1 (see figure 1) have a null dipole moment and vertices in topology T_2 have a finite dipole moment. Moreover, in the pyrochlore lattice a crystallization of vertice's dipole moments occurs only for very low temperatures, below the spin ice regime [15], in such a way that in the ice regime their interaction is negligible, ensuring ground state degeneracy and residual entropy. In the artificial spin ice in a square lattice on the other hand, there is a significant interaction between vertice's dipole moments, in such a way that system's energetics is dominated by such interactions and ground state degeneracy is removed. As a consequence, monopoles in artificial spin ice interact by a Coulombian interaction added to a linear string potential [10], related to an observable string of dipoles pointing from one monopole to the other whose tension depends on system's geometry [8, 11, 12, 13]. Such a string is also present in the CSI [3] but it is non energetic.

From the fundamental point of view, one important question that can be posed is how the Coulombian interactions among monopole excitations modify system's properties. In ASI, string tension is dominant once the excitation energy depends linearly on the string length [10]. However, Coulombian interactions among monopoles is still present and may modify system's properties in a detectable way [16, 17]. Indeed, the monopole interpretation of excitations in ASI (including the Coulombian interaction between excitations) is a very well based theoretical assumption, but to our knowledge the is still no experimental measurement capable of confirm that in a real ASI system at a given temperature the interaction between excitations is the expected one. Then, proper measurement of the interaction between excitations is a crucial step towards the development new devices based on ASI. In addition, a deeper understanding of how modifications in monopoles charge or string tension modify system properties may contribute even further to unleash ASI full possibilities. Moreover, it may give more detailed clues on how modifications in geometry or other system properties reflect on modifications of the string tension and monopoles charge. As a way to look for such kind of modification a model to describe artificial spin ice where string tension and monopole charge can be continuously varied is in order.

In this paper we show that a dumbbell model can be transformed into an emergent model of vertex excitations which is suitable for artificial spin ice systems. This model incorporates vertices dipole moment and as a consequence it reproduces correctly systems excitations and main properties. In addition, it allows one to analyze separately the contributions of each kind of excitation or even to vary the monopoles charge keeping the string tension constant, making it possible to identify characteristics in systems properties that are due to the interaction between monopoles alone. By considering a simple magnetization reversal process for different artificial spin ice realizations, i.e, different magnitudes for the Coulombian interaction for a given string tension, we found that Coulombian interactions add asymmetries in monopoles population distribution in such a way that its presence can be inferred. This observation may be used to develop methods to experimentally measure interactions between monopole excitations. The paper is organized as follows. In section II we present the emergent vertex model, section III contains our results for the effects of Coulombian interactions on system's properties and section IV is devoted to final considerations and conclusions.

2. The emergent vertex model

As mentioned in the introduction, the main difference between the description of CSI and ASI systems by means of a resummed dumbbell model is related to the vertice's net dipole moment. While in the CSI all vertices satisfying the two-in two-out ice rule have the same dipole moment in magnitude, in the ASI one of the two possible kind of vertices that satisfy the ice rule (topology T_1 in figure 1) has null dipole moment while the other (topology T_2 in figure 1) has a non-zero dipole moment. This difference introduces substantial modifications in the system behavior. In the ice regime of CSI the net charge of a tetrahedra (vertices) is the only relevant degree of freedom [3]. This means that the interaction between vertices' dipole moments are negligible and must not be considered. Then, using dumbbells, performing a resummation at vertices and properly setting creation energies for monopoles, an accurate description of systems' properties is obtained. In the ASI, the vertices' dipole moment cannot be neglected in order to obtain the ground state and low energy excitations. Indeed, since a creation energy can be attributed to the dipole moment of a vertex, one should expect that the ground state is the one with null net charge and null net dipole moment at each vertex, i.e., only vertices on topology T_1 composes the ground state as indeed is the case. As a consequence, excitations above the ordered ground state in ASI are described by the Coulombian interaction among monopoles (vertices that violate the ice rule, pertaining to topology T_3) added to a linear string potential related to the creation of vertices on topology T_2 that connect the monopoles as they are separated [10]. Following this reasoning, a dumbbell model suitable for ASI should incorporate vertices' dipole moment as well as its monopole moment.

In the conventional dumbbell picture used by Castelnovo et al [3], point charges of magnitude q separated by the lattice spacing, a, are used to replace point dipoles located in the midpoint along the line that connects the center of adjacent vertices. In addition, q is set such that $qa = \mu$, where μ is the dipole moment of the spins in the original point dipole model. Then, at each vertex, only a net monopole moment survives when all point dipoles are replaced by physical dipoles and a resummation is performed. In other approach [14, 18], the distance between monopoles in the dumbbell is set to the island length, which is smaller than the lattice spacing. Here, the distance between the dumbbell charges (d), or the monopole (Q) and dipole moments (p) of emergent vertices, will be fitted to provide the

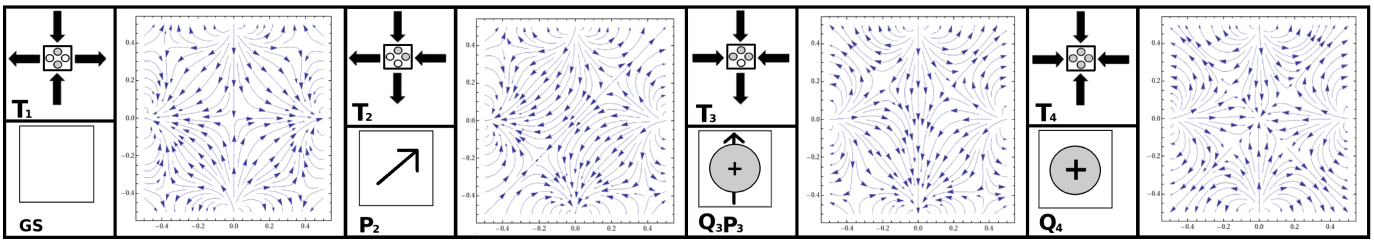

Figure 1: Topologies of the artificial square spin ice ordered according to increasing energy from left to right. Small boxes shows on the top the point dipoles (arrows) and dumbbell charges (circles) inside a square representing the vertex. The vertex side length is $l = a - d$, where a is the lattice spacing and d the dumbbell length. Gray circles represent positive (north) charges while white circles stand for negative (south) charges. The resulting charge and dipole moment of the vertex in the emergent model are shown on the small bottom boxes. T1 vertices have null charge and dipole moment, T2 vertices have null charge and a net dipole moment $P_2 = \sqrt{2}ql$, T3 vertices have total charge $Q_3 = \pm 2q$ and dipole moment $P_3 = 1ql$ and T4 vertices have total charge $Q_4 = \pm 4q$ and null dipole moment. Big boxes shows streamlines representing the magnetic field of the point dipoles. By looking to the corners the dipole moment direction can be inferred.

same energy difference between configurations of a point dipole model. In this picture, the monopole and the dipole moments are given, respectively, by $\sum_{k=1}^{4} q_k$ and $\sum_{k=1}^{4} q_k \cdot \vec{r}_k$, where q_k is the charge from spin k and $\vec{r}_k$ is its position measured from the vertex center. The key point is that by proper choice of these values, different realizations of ASI can be recovered. For example, the differences between two ASI realizations using islands with different widths, where one should expect to observe different dipole moments and monopole charges for excitations, can, in principle, be recovered while in other approaches (e.g. Refs.[14, 18]) this is not possible.

In figure 1 we show the vertex topologies and the corresponding dumbbell charges of a vertex (small boxes on the top), emergent vertices (small boxes on the bottom) and field streamlines (on the right) for an artificial square spin ice (ASSI). It seems at first sight, i.e., by looking only to the original and emergent vertices (top and bottom boxes in figure 1), that the dipole moments of the emergent vertices are pointing in the wrong direction. However, a closer inspection of the direction of the magnetic field produced by the point dipoles on the edges of the vertex, more specifically at the corners, shows that they should point as show on the middle panel of figure 1. Moreover, agreement between energies of the emergent and point dipoles models can only be obtained by considering them in this way. Other relevant point we can notice is that related to T_3 vertices there is a composite excitation that has charge and dipole moment. To our knowledge the dipole moment of this excitation was neglected in emergent models so far. This may be related to the fact that since the dipole moment, p, is small, the dipole field is much smaller than the monopole field, hiding its dipole character. Moreover, the main effect of such dipole moment would be to introduce anisotropies in the interactions that are likely to be hidden by the discrete symmetry of the square lattice where they live in.

Now that we have defined the excitations of the emergent model we can proceed to determine creation energies related to each vertex type and their monopole and dipole moments magnitude. At this point we must emphasize that different values for these constants leads to systems with very different physical properties. Indeed, for some values it may have absolutely no resemblance to an ASI. Is the proper choice of these values that guarantee that we are dealing with the desired system. Then, in order to obtain values that are suitable for an artificial square spin ice, we have used 10^6 configurations obtained from a Monte Carlo simulation of the ASSI using point dipoles as a benchmark. We used the conventional Metropolis algorithm[19] in a 34×34 lattice with open boundary conditions and dipolar interactions,

$$H_{pd} = D \sum_{i<j} \left[\frac{\vec{s}_i \cdot \vec{s}_j - 3(\vec{s}_i \cdot \hat{r}_{ij}) \cdot (\vec{s}_j \cdot \hat{r}_{ij})}{r_{ij}^3} \right],$$

where $D = \frac{\mu_0 \mu^2}{4\pi a^3}$ is the dipolar constant, μ is the island's dipole moment, a the lattice spacing and $\vec{s}_i$ and $\vec{r}_{ij}$ are the dimensionless dipole moment of site i and distance between sites i and j, respectively. The considered 10^6 configurations were obtained after thermalization for temperatures between 4 and 20 D/k_B. The ASSI has a phase transition at $T \approx 7D/k_B$ [20] and $T = 4D/k_B$ is a temperature low enough to allow proper sampling of the low temperature behavior of the system, including its ground-state. The energies obtained by using the point dipole model were renormalized to get null energy for the ground state, allowing better comparison to the emergent model. For each of these configurations the corresponding emergent vertices were obtained, allowing the computation of its energy as described by the following hamiltonian:

$$\begin{aligned} H_v &= \frac{\mu_0 q^2}{4\pi a} \sum_{i<j} \frac{Q_i Q_j}{r_{ij}} - \frac{\mu_0 q^2 l}{4\pi a^2} \sum_{i<j} \frac{\vec{p}_i \cdot \hat{r}_{ij}}{r_{ij}^2} \\ &+ \frac{\mu_0 q^2 l^2}{4\pi a^3} \sum_{i<j} \left[\frac{\vec{p}_i \cdot \vec{p}_j - 3(\vec{p}_i \cdot \hat{r}_{ij}) \cdot (\vec{p}_j \cdot \hat{r}_{ij})}{r_{ij}^3} \right] \\ &+ E_c^{T_2} \sum_i \delta_{i,T_2} + E_c^{T_3} \sum_i \delta_{i,T_3} \\ &+ E_c^{T_4} \sum_i \delta_{i,T_4}. \end{aligned} \quad (1)$$

In this expression, we introduced a dimensionless charge for vertex i, $Q_i = 0$ if vertex i is on topology T_1 or T_2, $Q_i = \pm 2$ if it is on topology T_3 and $Q_i = \pm 4$ if it is on topology T_4. The dimensionless dipole moment of vertex i is $|\vec{p}_i| = 0$ if it is on topology T_1 or T_4, $|\vec{p}_i| = 1$ if it is on topology T_3 and $|\vec{p}_i| = \sqrt{2}$ if it is on topology T_2. $E_c^{T_j}$ is the creation energy of a vertex

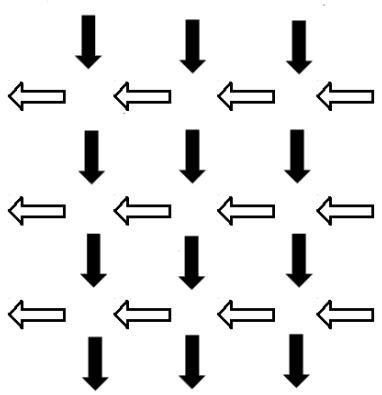

Figure 2: Initial configuration of the artificial square spin ice (ASSI) used in our simulations. By applying a magnetic field in the x direction only spins represented by open arrows flip. At each vertex the corresponding excitation of the emergent vertex model is obtained and used to calculate the magnetic field.

Table 1: Results of the least squares fit of the energies obtained from the point dipole model to equation 1. The last two lines show the R^2 and the standard deviation of the residuals, σ_E.

	Border excitation			
	Neglected		Considered	
	ql constrained to μ		ql constrained to μ	
Quantity	No	Yes	No	Yes
q	1.1451(4)	1.2169(4)	1.5199(1)	1.4855(1)
l	0.2579(3)	0.1781(3)	0.31592(5)	0.3268(5)
ql	0.2953(3)	0.2167(4)	0.48017(6)	0.4855(1)
$E_c^{T_2}$	10.392(1)	10.2066(9)	10.6642(3)	10.7061(3)
$E_c^{T_3}$	17.752(2)	17.893(3)	20.698(1)	20.486(1)
$E_c^{T_4}$	49.96(1)	50.60(1)	61.509(5)	60.605(4)
R^2	0.999977	0.999974	0.999998	0.999998
σ_E	18.19033	19.27400	4.891123	5.215461

on topology T_j (measured in units of D) and $\delta_{i,T_j} = 1$ if vertex i is on topology T_j and 0 otherwise. q is the magnitude of the dumbbell charge (measured in units of μ/a) and $m = ql$ gives the magnitude of the dipole moment of a vertex (see figure 1 for more details). The first term represents the interactions among monopoles, the second the interactions among monopoles and dipoles, the third interactions among dipoles and the last three terms represent the creation energy of each kind of vertex. As can be seen, the creation energy of a vertex on topology T_1 was set to zero, in such a way that for the ground-state, i.e., a state composed only by T_1 vertices the energy is zero.

The constants in the expression above (Eq. 1) has to be adjusted to give reasonable values for the energy. Indeed, without the values of the constants, q, l (measured in units of a) and $E_c^{T_j}$, this expression is meaningless since only the remaining parts of the expression can be obtained from the system configuration. In order to obtain the values of these constants we performed a least squares fit using the energy obtained from the point dipole model as dependent variable and equation 1 to predict its value by adjusting q, l and $E_c^{T_j}$. The assumption is that both models give the same energies for the same configurations or, at least, the energy difference between two configurations is the same for both models (point dipoles and emergent vertex model).

Before proceeding to the estimation of the emergent vertex model constants we have to deal with the border vertices. Vertices located at the system's boundary have less spins than the others, in such a way that the excitations related to them are different from the ones we are more interested in obtain. Then, we can take into account their excitations following the same procedure described for the remaining vertices or neglect their contribution. In order to simplify the possible border excitations, the ASSI lattice was build as shown in 2, in such a way that all border vertices have the same kind of excitation. Another point that have to be considered is if q and $l = a - d$ will be constrained to the island's dipole moment μ by doing $\mu = qd = q(a - l)$ or not. In table 1 we show results for the constants for all these possibilities. As can be seen by the analysis of the R^2 and standard deviation of residuals (σ_E), better results were obtained when the excitations at the borders were considered and q and l where not constrained to give the island's magnetic moment. However the obtained value, $qd \approx 1.04\mu$, is very close to the expected value $qd = \mu$.

To show further evidences of the equivalence between these two models we run Monte Carlo simulations of the emergent vertex model using the values contained in the third and fifth columns of table 1. A comparison between the energy, specific heat and magnetization of the pure dipole model and that of the emergent vertex model taking into account or not border excitations are shown in figure 3. As can be seen, there is complete agreement between these two models in the entire temperature range. The main differences between these two scenarios arise when we consider the population of each vertex type, shown in figure 4. Here we can see that by neglecting border excitations the populations are not well described. In summary, our best results indicates that border configurations should be considered while the differences introduced by constraining ql to μ may introduce only small modifications, expected to be irrelevant in comparison to thermal energy or imperfections present in real systems.

3. Analysis of vertex population in the magnetization reversal of ASSI

Signatures of the Coulombian interactions among monopoles in measurable quantities were investigated by using the emergent vertex model described in the last section in a magnetization reversal of the artificial square spin ice for different magnitudes of the monopole moment of the vertices. Note that this is equivalent to consider different ASSI realizations where the sole difference is the monopoles charge. Then, we placed spins, $\vec{S}_i$, on the sites of a square lattice of size $L = 64$ oriented along the x and y directions as in the ASSI, see figure 2. Each of these spins have an intrinsic barrier to flip, i.e., only when the component of total magnetic field on a spin that points in the opposite

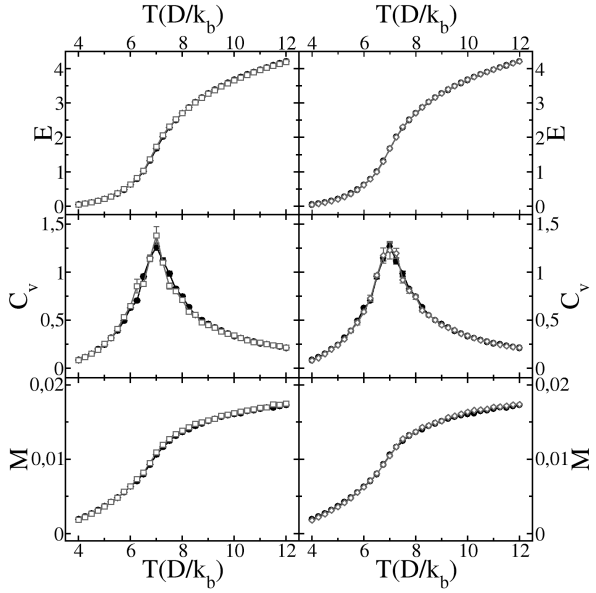

Figure 3: Comparison between Monte Carlo simulations of the point dipole model (full symbols) and the emergent vertex model (open symbols). On the left we used results from the third column of table 1 and on the right from the fifth column. From top to bottom we show the energy, specific heat and magnetization as a function of the temperature.

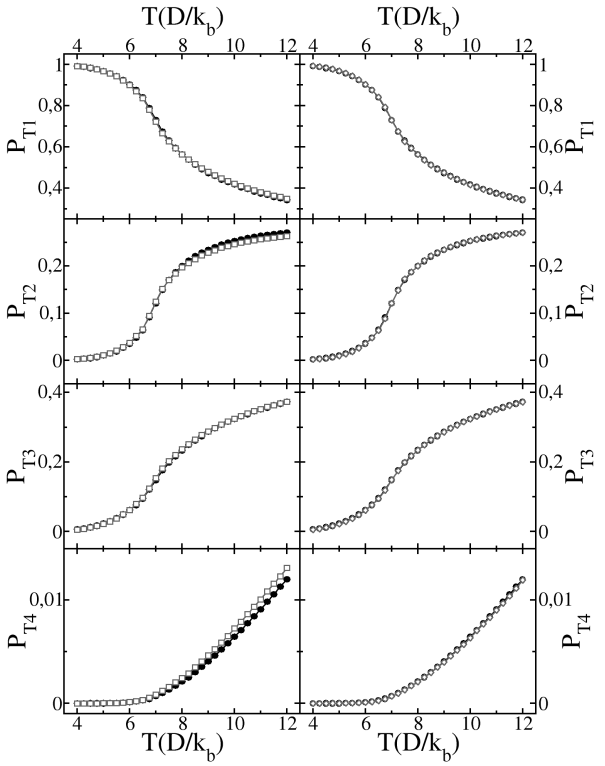

Figure 4: Comparison between Monte Carlo simulations of the point dipole model (full symbols) and the emergent vertex model (open symbols). On the left we used results from the third column of table 1 and on the right from the fifth column. From top to bottom we show the population of vertices T_1, T_2, T_3 and T_4 as a function of the temperature.

direction, $-\vec{B}_i^{Tot}\cdot\vec{S}_i$, exceeds a determined threshold, b_i, the spin flips [9, 21, 22]. In our procedure all spins are initially aligned in the negative x and y directions and an external uniform magnetic field, $\vec{B}^{ext}$, aligned in the positive x direction, is gradually applied, inducing the reversal of all horizontal spins. In addition to the external field we considered the field produced by the excitations that exist in each vertex as a consequence of the corresponding emergent vertex model, $\vec{B}_i^{vert}$, in the position of the spin i. Note that $\vec{B}_i^{vert}$ includes the contributions of all monopoles and dipoles of the emergent vertex model. So, the monopole and dipole moments of each excitation contribute to the flipping of a given spin, affecting the system behavior. Then, by varying the monopole moment magnitude keeping the dipole moment of each excitation fixed we can look for modifications in system properties produced by the Coulombian interaction alone. We have then fixed the magnitude of the dipole moment as $m = 0.5$, in accordance with the value shown in table 1 and varied the monopole charge q, between 0 and 10.

For a perfect system, in the sense that the reversal field for all spins is the same, all spins flip for the same value of the external field in a large enough system. But in real systems inhomogeneities in the nanoislands induces small variations in the reversal field [23, 24], introducing a quenched disorder in the system. This is incorporated in our model by considering that the reversal field, b_i follows a Normal distribution of standard deviation Δb centered at b_m [9, 22]. For simplicity we have set $b_m = 100$ and $\Delta b = 2.5$, 5, 10 and 15 in dimensionless units. For the simulation the external magnetic field, $|\vec{B}^{ext}|$, is slowly increased from 0 in steps of size 0.1. After each field step spins are randomly chosen and flipped if $-\vec{B}_i^{Tot}\cdot\vec{S}_i \leq b_i$. After $5\times N$ random choices, where N is the number of spins in the system, all spins of the system are tested according to the preceding equation and flipped if it is satisfied. After each spin flip the external field changes and the process is restarted.

In figure 5 we show results for the population of vertices in topologies T_2 and T_3 as a function of the external field for $q = 1.5$ and $\Delta b = 10$. The T_2 vertices were divided into two classes depending on the direction of its dipole moment. At the beginning, i.e., for the initial configuration, all dipoles point in the positive x direction, T_2^+. As the field increases spins are flipped and they change its dipole direction, starting to point in the negative x direction, T_2^-. This process is mediated by the creation and propagation of T_3 vertices (monopoles). These are the only types of vertices present in this simulation. Similar curves are obtained for all q values. However, one can notice small asymmetries in the distribution of monopoles as well as modifications in the position of the maxima and its height. In figure 6 we show in a) representative curves for the population of monopoles as a function of the external field, the maximum population of T_3 vertices (P_{max}) as a function of the monopole charge is shown in b), the distribution mode (X_0) in c) and the standard deviation (σ) in d). The open symbols were obtained considering all lattice sizes while full symbols were obtained by considering only the central portion of the system ($L/2\times L/2$) in a attempt to minimize border effects. As can be seen, these quantities diminishes for increasing monopole charge, being

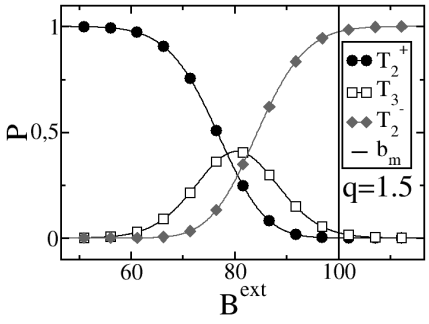

Figure 5: Vertex population as a function of the external field for $q = 1.5$.

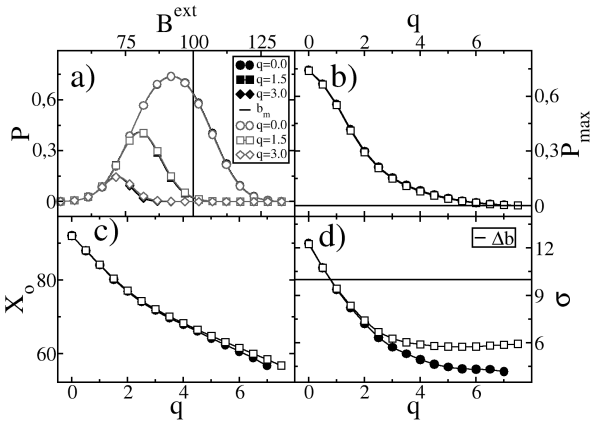

Figure 6: a) Monopole population as a function of the external field for $q = 0$, 1.5 and 3. b) Maximum population of monopoles as a function of the monopole charge, q. c) Monopole distribution mode, X_0 as a function of q. d) Standard deviation of the monopole distribution, σ, as a function of the monopole charge. Full symbols were obtained considering only the central part of the lattice while open symbols were obtained for all lattice sizes.

thus our first measurable evidence of the Coulombian interaction between monopoles. As can be seen, the field range were the transition occurs is approximately σ in such a way that for high enough q it occurs in a single field step. Thus, quantities of interest were obtained only when $P_{max} > 0.05$, ensuring a minimum population to obtain them.

Further evidences of Coulombian interactions can be obtained by analyzing the skewness and kurtosis [25, 26] of the monopoles distribution. In figure 7 we show the skewness coefficient,

$$K_s = \frac{m_3}{\sigma^3},$$

where m_3 is the third moment of the distribution and σ its standard deviation, and the excess kurtosis coefficient,

$$K_c = \frac{m_4}{\sigma^4} - 3,$$

were m_4 is the fourth moment of the distribution. Negative values of K_s indicate that the distribution is skewed left while positive values are related to a skewed right distribution. Using the above definition, $K_c = 0$ for the normal distribution. So, positive values of K_c indicate a platykurtic distribution while a

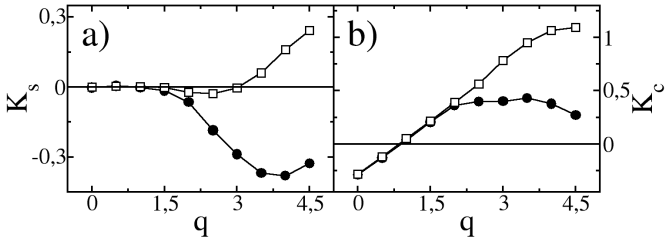

Figure 7: Skewness (a) and kurtosis (b) coefficients of the monopoles distribution as a function of the monopole charge. For large values of the monopole its distribution starts to be skewed left and leptokurtic. Full symbols were obtained considering only the central part of the lattice while open symbols were obtained for all lattice sizes.

negative value of K_c is related to a leptokurtic distribution. As can be seen (figure 7), the monopoles distribution tends to be skewed left and platykurtic for high values of q. In our previous analysis (see table 1) we found $q \approx 1.5$ for the point dipole model, approximately the value above which the distribution starts to have modified skewness and kurtosis coefficients. We believe that proper design of the nanoislands can be used to achieve monopole charges on the emergent vertex model above this value for which case the distribution curves will deviate from a normal distribution providing an indirect measurement of monopole charge.

The effect of different strengths of the disorder in the system is shown in figure 8 and 9. They indicate that even for relatively high degrees of disorder, as 15%, the analysis of skewness and kurtosis for the central portion of the system is capable to detect the Coulombian interactions among monopole excitations. As shown, the main effect is that appreciable deviations from the normal distribution appears for larger values of the monopole charge and mainly for the central portion of the system. In addition, an interesting feature is observed in the maximum population. As can be seen in figure 8 b), there is a crossing point of the curves, indicating that the population increases with decreasing disorder for q smaller than 1.5 and that decreases for decreasing disorder for q greater than 1.5. The same crossing point is found in the kurtosis coefficient curves in figure 9, in which for q smaller than 1.5 leptokurtic curves are obtained. We still do not have any reasonable explanation for this behavior and believe it deserves further investigations, however, this is out of the scope of this work.

Recent realizations of artificial spin ice systems [27, 28, 29, 30, 31] shows that proper engineering of nanoislands can be used to obtain thermal fluctuations at room temperature. This introduces fluctuations that were not considered in the above calculations. In order to introduce temperature effects in our simulations allowing the extension of our conclusions to thermal systems, we introduced a fluctuating magnetic field, $\vec{B}_i^t$ given by a normal distribution centered at zero and with standard deviation ΔB^t, in a way similar to what was done by Martinez *et al* [32]. Then, at each field step a new distribution of the thermal magnetic field is chosen. This is expected to cover situations were the external magnetic field changes in a time scale comparable to the time scale of relevant modifications in

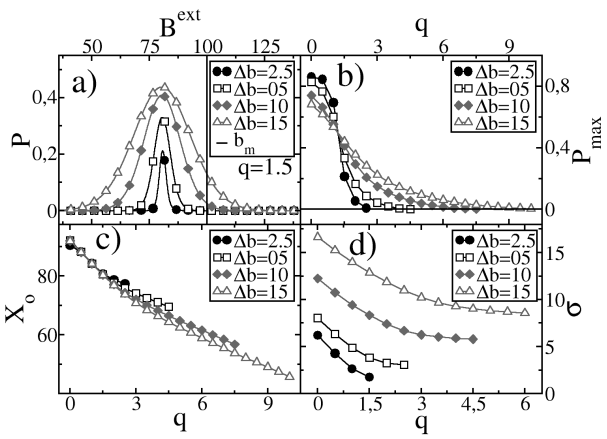

Figure 8: a) Monopole population as a function of the external field for different strengths of disorder as indicated in the legend. b) Maximum population of monopoles as a function of the monopole charge, q. c) Monopole distribution mode, X_0 as a function of q. d) Standard deviation of the monopole distribution, σ, as a function of the monopole charge.

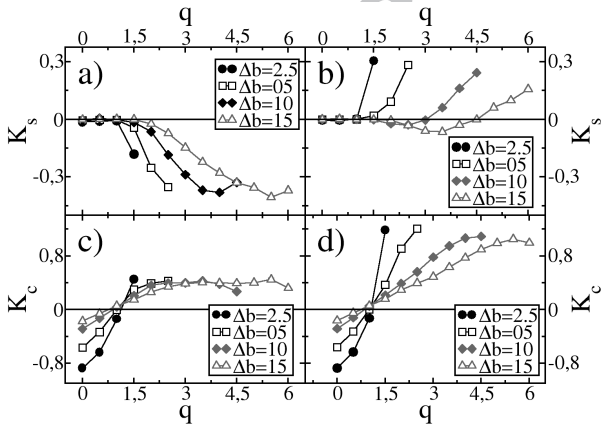

Figure 9: Skewness (a-b) and kurtosis (c-d) coefficients of the monopoles distribution as a function of the monopole charge for different disorders as indicated in the legend. On the left we show the results considering only the central portion of the system while on the right the results considering all sites is shown.

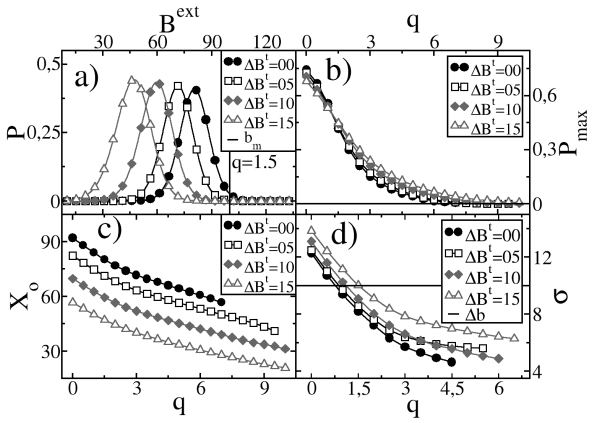

Figure 10: a) Monopole population as a function of the external field for different thermal field strengths as indicated in the legend. b) Maximum population of monopoles as a function of the monopole charge, q. c) Monopole distribution mode, X_0 as a function of q. d) Standard deviation of the monopole distribution, σ, as a function of the monopole charge.

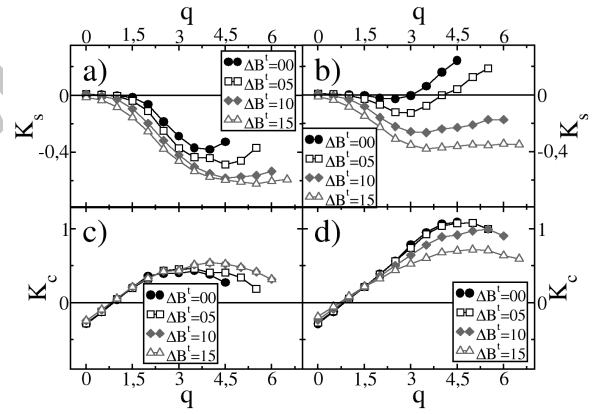

Figure 11: Skewness (a-b) and kurtosis (c-d) coefficients of the monopoles distribution as a function of the monopole charge for different strengths of the thermal field as indicated in the legend. On the left we show the results considering only the central portion of the system while on the right the results considering all sites is shown.

the reversal field of the islands due to thermal effects. Note that this is equivalent to consider random fluctuations on the reversal field of spins and on magnetic moments of emergent vertices. Of course, ΔB^t will be proportional to the system temperature. In figures 10 and 11 we show results for ΔB^t = 0, 5, 10 and 15 and for Δb = 10. As can be seen, only small quantitative differences are observed for the population, maximum population, mode and standard deviation of the distribution of monopoles (figure 10) as compared to the curves for different disorder strengths shown in figure 8. A qualitative difference is only observed for the skewness of monopoles distribution for the entire lattice that starts to be skewed left, while for increasing quench disorder it tends to be skewed right, making them easier to detect in experimental measurements, even for those with smaller magnitudes.

4. Conclusions

In this paper we have shown that an efficient emergent vertex model for artificial spin ice systems can be build by properly considering the dipole moments of vertex excitations. As we have shown, creation energies, monopoles charges and dipole moments can be properly fitted to a given ASI realization, yielding very satisfactory results as evidenced by the comparison between the Monte Carlo simulations of the point dipole and emergent models. It is worth recall that without proper consideration of vertices' dipole moments the description of system energetic fails and the use of emergent vertex models for ASI is limited.

The emergent vertex model we built allowed us to consider the signatures of Coulombian interactions among monopoles in the artificial square spin ice. We have shown that the skewness and kurtosis of monopoles distribution in a magnetization reversal process increases for increasing monopole charge. This constitute a direct measurable quantity easily accessible with modern experimental techniques, specially XMCD measurements. We expect that different ASSI realizations would result in different monopoles charges and thus different levels of skewness and kurtosis in monopoles distribution, evidencing the Coulombian character of monopoles interactions. We have also shown that this behavior is robust against the presence of disorder and thermal fluctuations, making it feasible for real experiments.

Regarding the emergent vertex model we would like to stress that one can use energies from a micromagnetic simulation, for example, instead of energies from the point dipole model to obtain creation energies and monopole and dipole moments that incorporates details about islands geometry and composition. Thus, we believe that this emergent model may constitute a very useful framework to study ASI systems in any geometry, allowing better comparison with experimental results with a much smaller computational effort. As shown, both, system dynamics and thermodynamics can be studied using it.

Acknowledgments

The authors gratefully acknowledge partial financial support from CNPq under grants 478220/2013-8 and 306457/2016-4 , FAPEMIG under grant PPM-00204-14 and CAPES.

References

[1] M. J. Harris, S. T. Bramwell, D. F. McMorrow, T. Zeiske, K. W. Godfrey, Geometrical frustration in the ferromagnetic pyrochlore $ho_2ti_2O_7$, Phys. Rev. Lett. 79 (1997) 2554–2557. doi:10.1103/PhysRevLett.79.2554.
URL https://link.aps.org/doi/10.1103/PhysRevLett.79.2554

[2] S. T. Bramwell, M. J. P. Gingras, Spin ice state in frustrated magnetic pyrochlore materials, Science 294 (5546) (2001) 1495–1501. arXiv:http://science.sciencemag.org/content/294/5546/1495.full.pdf, doi:10.1126/science.1064761.
URL http://science.sciencemag.org/content/294/5546/1495

[3] C. Castelnovo, R. Moessner, S. L. Sondhi, Magnetic monopoles in spin ice, Nature 451 (7174) (2008) 42–45. doi:10.1038/nature06433.
URL http://dx.doi.org/10.1038/nature06433

[4] R. F. Wang, C. Nisoli, R. S. Freitas, J. Li, W. McConville, B. J. Cooley, M. S. Lund, N. Samarth, C. Leighton, V. H. Crespi, P. Schiffer, Artificial 'spin ice' in a geometrically frustrated lattice of nanoscale ferromagnetic islands, Nature 439 (7074) (2006) 303–306. doi:10.1038/nature04447.
URL http://dx.doi.org/10.1038/nature04447

[5] C. Nisoli, R. Moessner, P. Schiffer, *Colloquium*: Artificial spin ice: Designing and imaging magnetic frustration, Rev. Mod. Phys. 85 (2013) 1473–1490. doi:10.1103/RevModPhys.85.1473.
URL https://link.aps.org/doi/10.1103/RevModPhys.85.1473

[6] M. Tanaka, E. Saitoh, H. Miyajima, T. Yamaoka, Y. Iye, Magnetic interactions in a ferromagnetic honeycomb nanoscale network, Phys. Rev. B 73 (2006) 052411. doi:10.1103/PhysRevB.73.052411.
URL https://link.aps.org/doi/10.1103/PhysRevB.73.052411

[7] E. Mengotti, L. J. Heyderman, A. F. Rodriguez, F. Nolting, R. V. Hugli, H.-B. Braun, Real-space observation of emergent magnetic monopoles and associated dirac strings in artificial kagome spin ice, Nat Phys 7 (1) (2011) 68–74. doi:10.1038/nphys1794.
URL http://dx.doi.org/10.1038/nphys1794

[8] L. A. S. Mól, A. R. Pereira, W. A. Moura-Melo, Extending spin ice concepts to another geometry: The artificial triangular spin ice, Phys. Rev. B 85 (2012) 184410. doi:10.1103/PhysRevB.85.184410.
URL https://link.aps.org/doi/10.1103/PhysRevB.85.184410

[9] J. H. Rodrigues, L. A. S. Mól, W. A. Moura-Melo, A. R. Pereira, Efficient demagnetization protocol for the artificial triangular spin ice, Applied Physics Letters 103 (9) (2013) 092403. arXiv:http://dx.doi.org/10.1063/1.4819844, doi:10.1063/1.4819844.
URL http://dx.doi.org/10.1063/1.4819844

[10] L. A. Mól, R. L. Silva, R. C. Silva, A. R. Pereira, W. A. Moura-Melo, B. V. Costa, Magnetic monopole and string excitations in two-dimensional spin ice, Journal of Applied Physics 106 (6) (2009) 063913. arXiv:http://dx.doi.org/10.1063/1.3224870, doi:10.1063/1.3224870.
URL http://dx.doi.org/10.1063/1.3224870

[11] L. A. S. Mól, W. A. Moura-Melo, A. R. Pereira, Conditions for free magnetic monopoles in nanoscale square arrays of dipolar spin ice, Phys. Rev. B 82 (2010) 054434. doi:10.1103/PhysRevB.82.054434.
URL https://link.aps.org/doi/10.1103/PhysRevB.82.054434

[12] F. S. Nascimento, L. A. S. Mól, W. A. Moura-Melo, A. R. Pereira, From confinement to deconfinement of magnetic monopoles in artificial rectangular spin ices, New Journal of Physics 14 (11) (2012) 115019.
URL http://stacks.iop.org/1367-2630/14/i=11/a=115019

[13] R. P. Loreto, L. A. Morais, C. I. L. de Araujo, W. A. Moura-Melo, A. R. Pereira, R. C. Silva, F. S. Nascimento, L. A. S. Mól, Emergence and mobility of monopoles in a unidirectional arrangement of magnetic nanoislands, Nanotechnology 26 (29) (2015) 295303.
URL http://stacks.iop.org/0957-4484/26/i=29/a=295303

[14] G. Möller, R. Moessner, Artificial square ice and related dipolar nanoarrays, Phys. Rev. Lett. 96 (2006) 237202. doi:10.1103/PhysRevLett.96.237202.
URL https://link.aps.org/doi/10.1103/PhysRevLett.96.237202

[15] R. G. Melko, M. J. P. Gingras, Monte carlo studies of the dipolar spin ice model, Journal of Physics: Condensed Matter 16 (43) (2004) R1277.
URL http://stacks.iop.org/0953-8984/16/i=43/a=R02

[16] A. León, Heavy and light monopoles in magnetic reversion in artificial spin ice, Current Applied Physics 13 (9) (2013) 2014 – 2018. doi:http://dx.doi.org/10.1016/j.cap.2013.08.010.
URL http://www.sciencedirect.com/science/article/pii/S1567173913003027

[17] A. León, Thermal phase transition in artificial spin ice systems induces the formation and migration of monopole-like magnetic excitations, Physica B: Condensed Matter 500 (2016) 59 – 65. doi:http://dx.doi.org/10.1016/j.physb.2016.07.012.
URL http://www.sciencedirect.com/science/article/pii/

S0921452616302903

[18] G. Möller, R. Moessner, Magnetic multipole analysis of kagome and artificial spin-ice dipolar arrays, Phys. Rev. B 80 (2009) 140409. doi:10.1103/PhysRevB.80.140409.
URL https://link.aps.org/doi/10.1103/PhysRevB.80.140409

[19] D. P. Landau, K. Binder, A Guide to Monte Carlo Simulations in Statistical Physics, 4th Edition, Cambridge University Press, 2014. doi:10.1017/CBO9781139696463.

[20] R. C. Silva, F. S. Nascimento, L. A. S. Mól, W. A. Moura-Melo, A. R. Pereira, Thermodynamics of elementary excitations in artificial magnetic square ice, New Journal of Physics 14 (1) (2012) 015008.
URL http://stacks.iop.org/1367-2630/14/i=1/a=015008

[21] Z. Budrikis, P. Politi, R. L. Stamps, Vertex dynamics in finite two-dimensional square spin ices, Phys. Rev. Lett. 105 (2010) 017201. doi:10.1103/PhysRevLett.105.017201.
URL https://link.aps.org/doi/10.1103/PhysRevLett.105.017201

[22] Z. Budrikis, P. Politi, R. L. Stamps, Diversity enabling equilibration: Disorder and the ground state in artificial spin ice, Phys. Rev. Lett. 107 (2011) 217204. doi:10.1103/PhysRevLett.107.217204.
URL https://link.aps.org/doi/10.1103/PhysRevLett.107.217204

[23] K. K. Kohli, A. L. Balk, J. Li, S. Zhang, I. Gilbert, P. E. Lammert, V. H. Crespi, P. Schiffer, N. Samarth, Magneto-optical kerr effect studies of square artificial spin ice, Phys. Rev. B 84 (2011) 180412. doi:10.1103/PhysRevB.84.180412.
URL https://link.aps.org/doi/10.1103/PhysRevB.84.180412

[24] S. D. Pollard, V. Volkov, Y. Zhu, Propagation of magnetic charge monopoles and dirac flux strings in an artificial spin-ice lattice, Phys. Rev. B 85 (2012) 180402. doi:10.1103/PhysRevB.85.180402.
URL https://link.aps.org/doi/10.1103/PhysRevB.85.180402

[25] M. J. Bulmer, Principles of Statistics, 1st Edition, Dover Publications, Inc, 1979.

[26] D. K. Hildebrand, Statistical Thinking for Behavioral Scientists, 1st Edition, Duxbury Press, 1986.

[27] J. P. Morgan, A. Stein, S. Langridge, C. H. Marrows, Thermal ground-state ordering and elementary excitations in artificial magnetic square ice, Nat Phys 7 (1) (2011) 75–79. doi:10.1038/nphys1853.
URL http://dx.doi.org/10.1038/nphys1853

[28] V. Kapaklis, U. B. Arnalds, A. Farhan, R. V. Chopdekar, A. Balan, A. Scholl, L. J. Heyderman, B. Hjorvarsson, Thermal fluctuations in artificial spin ice, Nat Nano 9 (7) (2014) 514–519, letter.
URL http://dx.doi.org/10.1038/nnano.2014.104

[29] D. Thonig, S. ReiBaus, I. Mertig, J. Henk, Thermal string excitations in artificial spin-ice square dipolar arrays, Journal of Physics: Condensed Matter 26 (26) (2014) 266006.
URL http://stacks.iop.org/0953-8984/26/i=26/a=266006

[30] A. Farhan, A. Scholl, C. F. Petersen, L. Anghinolfi, C. Wuth, S. Dhuey, R. V. Chopdekar, P. Mellado, M. J. Alava, S. van Dijken, Thermodynamics of emergent magnetic charge screening in artificial spin ice, Nature Communications 7 (2016) 12635 EP –.
URL http://dx.doi.org/10.1038/ncomms12635

[31] K. Zeissler, M. Chadha, E. Lovell, L. F. Cohen, W. R. Branford, Low temperature and high field regimes of connected kagome artificial spin ice: the role of domain wall topology, Scientific Reports 6 (2016) 30218 EP –.
URL http://dx.doi.org/10.1038/srep30218

[32] E. Martinez, L. Lopez-Diaz, L. Torres, C. Garcia-Cervera, Thermal activation in permalloy nanorectangles at room temperature, Physica B: Condensed Matter 372 (1) (2006) 286 – 289, proceedings of the Fifth International Symposium on Hysteresis and Micromagnetic Modeling. doi:http://dx.doi.org/10.1016/j.physb.2005.10.068.
URL http://www.sciencedirect.com/science/article/pii/S092145260501104X